ISSN 1948-9366 (online)

World Journal of

Gastrointestinal Surgery

World J Gastrointest Surg 2023 May 27; 15(5): 745-1006

Published by Baishideng Publishing Group Inc

World Journal of Gastrointestinal Surgery

Contents

Monthly Volume 15 Number 5 May 27, 2023

World Journal of Gastrointestinal Surgery

Monthly Volume 15 Number 5 May 27, 2023

Contents

World Journal of Gastrointestinal Surgery

Monthly Volume 15 Number 5 May 27, 2023

Contents

ABOUT COVER

Editorial Board Member of *World Journal of Gastrointestinal Surgery*, Ashok Kumar, BSc, FACS, FASCRS, FICS, FRCS, FRCS (Ed), MBBS, MCh, Professor, Department of Surgical Gastroenterology, Sanjay Gandhi Post Graduate Institute of Medical Sciences, Lucknow 226014, Uttar Pradesh, India. doc.ashokgupta@gmail.com

AIMS AND SCOPE

The primary aim of *World Journal of Gastrointestinal Surgery* (*WJGS*, *World J Gastrointest Surg*) is to provide scholars and readers from various fields of gastrointestinal surgery with a platform to publish high-quality basic and clinical research articles and communicate their research findings online.

WJGS mainly publishes articles reporting research results and findings obtained in the field of gastrointestinal surgery and covering a wide range of topics including biliary tract surgical procedures, biliopancreatic diversion, colectomy, esophagectomy, esophagostomy, pancreas transplantation, and pancreatectomy, *etc*.

INDEXING/ABSTRACTING

The *WJGS* is now abstracted and indexed in Science Citation Index Expanded (SCIE, also known as SciSearch®), Current Contents/Clinical Medicine, Journal Citation Reports/Science Edition, PubMed, PubMed Central, Reference Citation Analysis, China National Knowledge Infrastructure, China Science and Technology Journal Database, and Superstar Journals Database. The 2022 Edition of Journal Citation Reports® cites the 2021 impact factor (IF) for *WJGS* as 2.505; IF without journal self cites: 2.473; 5-year IF: 3.099; Journal Citation Indicator: 0.49; Ranking: 104 among 211 journals in surgery; Quartile category: Q2; Ranking: 81 among 93 journals in gastroenterology and hepatology; and Quartile category: Q4.

RESPONSIBLE EDITORS FOR THIS ISSUE

Production Editor: *Rui-Rui Wu*; **Production Department Director:** *Xiang Li*; **Editorial Office Director:** *Jia-Ru Fan*.

NAME OF JOURNAL
World Journal of Gastrointestinal Surgery

ISSN
ISSN 1948-9366 (online)

LAUNCH DATE
November 30, 2009

FREQUENCY
Monthly

EDITORS-IN-CHIEF
Peter Schemmer

EDITORIAL BOARD MEMBERS
https://www.wjgnet.com/1948-9366/editorialboard.htm

PUBLICATION DATE
May 27, 2023

INSTRUCTIONS TO AUTHORS
https://www.wjgnet.com/bpg/gerinfo/204

GUIDELINES FOR ETHICS DOCUMENTS
https://www.wjgnet.com/bpg/GerInfo/287

GUIDELINES FOR NON-NATIVE SPEAKERS OF ENGLISH
https://www.wjgnet.com/bpg/gerinfo/240

PUBLICATION ETHICS
https://www.wjgnet.com/bpg/GerInfo/288

PUBLICATION MISCONDUCT
https://www.wjgnet.com/bpg/gerinfo/208

ARTICLE PROCESSING CHARGE
https://www.wjgnet.com/bpg/gerinfo/242

STEPS FOR SUBMITTING MANUSCRIPTS
https://www.wjgnet.com/bpg/GerInfo/239

ONLINE SUBMISSION
https://www.f6publishing.com

World Journal of Gastrointestinal Surgery

Submit a Manuscript: https://www.f6publishing.com

World J Gastrointest Surg 2023 May 27; 15(5): 882-891

DOI: 10.4240/wjgs.v15.i5.882

ISSN 1948-9366 (online)

ORIGINAL ARTICLE

Retrospective Study

Diagnostic performance of texture analysis in the differential diagnosis of perianal fistulising Crohn's disease and glandular anal fistula

Xin Zhu, Dan-Dan Ye, Jian-Hua Wang, Jing Li, Shao-Wei Liu

Specialty type: Gastroenterology and hepatology

Provenance and peer review: Unsolicited article; Externally peer reviewed.

Peer-review model: Single blind

Peer-review report's scientific quality classification

Grade A (Excellent): 0
Grade B (Very good): B
Grade C (Good): C
Grade D (Fair): D
Grade E (Poor): 0

P-Reviewer: Aydin S, Turkey; Choi YS, South Korea; Garg P, India

Received: December 12, 2022
Peer-review started: December 12, 2022
First decision: January 2, 2023
Revised: January 16, 2023
Accepted: March 30, 2023
Article in press: March 30, 2023
Published online: May 27, 2023

Xin Zhu, Jian-Hua Wang, Jing Li, Shao-Wei Liu, Department of Radiology, Affiliated Hospital of Nanjing University of Chinese Medicine, Nanjing 210029, Jiangsu Province, China

Dan-Dan Ye, Department of Radiology, Quanzhou Orthopedic-Traumatological Hospital, Quanzhou 362000, Fujian Province, China

Corresponding author: Xin Zhu, Doctor, MD, Chief Doctor, Department of Radiology, Affiliated Hospital of Nanjing University of Chinese Medicine, No. 155 Hanzhong Road, Nanjing 210029, Jiangsu Province, China. zhuxin-njcm@njucm.edu.cn

Abstract

BACKGROUND

Perianal fistulising Crohn's disease (PFCD) and glandular anal fistula have many similarities on conventional magnetic resonance imaging. However, many patients with PFCD show concomitant active proctitis, but only few patients with glandular anal fistula have active proctitis.

AIM

To explore the value of differential diagnosis of PFCD and glandular anal fistula by comparing the textural feature parameters of the rectum and anal canal in fat suppression T2-weighted imaging (FS-T2WI).

METHODS

Patients with rectal water sac implantation were screened from the first part of this study (48 patients with PFCD and 22 patients with glandular anal fistula). Open-source software ITK-SNAP (Version 3.6.0, http://www.itksnap.org/) was used to delineate the region of interest (ROI) of the entire rectum and anal canal wall on every axial section, and then the ROIs were input in the Analysis Kit software (version V3.0.0.R, GE Healthcare) to calculate the textural feature parameters. Textural feature parameter differences of the rectum and anal canal wall between the PFCD group *vs* the glandular anal fistula group were analyzed using Mann-Whitney U test. The redundant textural parameters were screened by bivariate Spearman correlation analysis, and binary logistic regression analysis was used to establish the model of textural feature parameters. Finally, diagnostic accuracy was assessed by receiver operating characteristic-area under the curve (AUC) analysis.

RESULTS

In all, 385 textural parameters were obtained, including 37 parameters with statistically significant differences between the PFCD and glandular anal fistula groups. Then, 16 texture feature parameters remained after bivariate Spearman correlation analysis, including one histogram parameter (Histogram energy); four grey level co-occurrence matrix (GLCM) parameters (GLCM energy_all direction_offset1_SD, GLCM entropy_all direction_ offset4_SD, GLCM entropy_all direction_offset7_SD, and Haralick correlation_all direction_ offset7_SD); four texture parameters (Correlation_all direction_offset1_SD, cluster prominence _angle 90_offset4, Inertia_all direction_offset7_SD, and cluster shade_angle 45_offset7); five grey level run-length matrix parameters (grey level nonuniformity_angle 90_offset1, grey level nonuniformity_all direction_offset4_SD, long run high grey level emphasis_all direction_offset1_SD, long run emphasis_all direction_ offset4_ SD, and long run high grey level emphasis_all direction_offset4_SD); and two form factor parameters (surface area and maximum 3D diameter). The AUC, sensitivity, and specificity of the model of textural feature parameters were 0.917, 85.42%, and 86.36%, respectively.

CONCLUSION

The model of textural feature parameters showed good diagnostic performance for PFCD. The texture feature parameters of the rectum and anal canal in FS-T2WI are helpful to distinguish PFCD from glandular anal fistula.

Key Words: Anal fistula; Crohn's diseases; Magnetic resonance imaging; Texture analysis; Differential diagnosis

Core Tip: Crohn's disease (CD) is a localized, segmental chronic granulomatous inflammation that can affect the digestive tract from the oral cavity to the anus, and its pathophysiology is non-caseous necrotic granuloma. Nearly 10% of patients with CD have an anal fistula before presenting gastrointestinal symptoms. At the same time, perianal fistulising CD (PFCD) and glandular anal fistula have many similarities on conventional magnetic resonance imaging (MRI); therefore, it is difficult to differentiate between these conditions in the early stages with conventional MRI. Texture analysis based on conventional MRI images can quantitatively analyze image pixel information and reflect the internal heterogeneity and pathological characteristics of the lesion. Currently, this approach is widely used to distinguish between benign and malignant tumors, predict tumor stage, and evaluate treatment efficacy. In addition to the application of texture analysis in the study of tumors or substantial organs, some studies have applied texture analysis to hollow organs such as the intestine. Many patients with PFCD show concomitant active proctitis, but only few patients with glandular anal fistula have active proctitis. Based on this theory, we analyzed the texture of the rectum and anal canal wall in the PFCD group and glandular anal fistula group in this study to explore whether the texture feature parameters are valuable in identifying and differentiating these two lesions.

Citation: Zhu X, Ye DD, Wang JH, Li J, Liu SW. Diagnostic performance of texture analysis in the differential diagnosis of perianal fistulising Crohn's disease and glandular anal fistula. *World J Gastrointest Surg* 2023; 15(5): 882-891

URL: https://www.wjgnet.com/1948-9366/full/v15/i5/882.htm

DOI: https://dx.doi.org/10.4240/wjgs.v15.i5.882

INTRODUCTION

Crohn's disease (CD) is a localized, segmental chronic granulomatous inflammation that can affect the digestive tract from the oral cavity to the anus, and its pathophysiology is non-caseous necrotic granuloma[1]. Nearly 10% patients with CD have an anal fistula before presenting with gastrointestinal symptoms. At the same time, perianal fistulising CD (PFCD) and glandular anal fistula have many similarities on conventional magnetic resonance imaging (MRI); therefore, it is difficult to differentiate these conditions in the early stages with conventional MRI[2]. Texture analysis based on conventional MRI images can quantitatively analyze image pixel information and reflect the internal heterogeneity and pathological characteristics of the lesion[3]. Currently, this approach is widely used to distinguish between benign and malignant tumors, predict tumor stage, and evaluate treatment efficacy[4-7]. In

addition to the application of texture analysis in the study of tumors or substantial organs, some studies have applied texture analysis to hollow organs such as the intestine[8,9]. Many patients with PFCD show concomitant active proctitis, but only few patients with glandular anal fistula have active proctitis. Based on this theory, we analyzed the texture of the rectum and anal canal wall in the PFCD group and glandular anal fistula group in this study to explore whether the texture feature parameters are valuable in identifying and differentiating these two lesions.

MATERIALS AND METHODS

General data

This study was approved by the institutional review board of the Affiliated Hospital of Nanjing University of Chinese Medicine; informed consent was waived owing to the retrospective nature of the study. This study was conducted in two parts through a search of our medical records. In the first part, we conducted screening for rectal water sac implantation in the existing cohort of PFCD and glandular anal fistula patients; those with an air sac or water sac were included and those without, were excluded. The flow chart of patient inclusion and exclusion is shown in Figure 1. Finally, 48 PFCD patients [41 male and 7 female; mean age: 28.60 ± 10.77 (13–61) years] with rectal water sac implantation were screened. Of these, 22 patients [19 male and 3 female; mean age: 34.95 ± 12.71 (15–62) years] had glandular anal fistula with rectal water sac implantation. This study was approved by the Ethics Review Committee of our hospital. Considering the retrospective nature of the study, the need for informed consent was waived.

MRI examination method

Before MRI examination of the rectum, the patient was required to perform cleansing enema, and a water sac (approximately 150 mL of normal saline, fully expanded) was inserted into the rectal cavity by the clinician. All MRI exams were performed using a Siemens Magnetom Aera 1.5 T scanner, and the body phased array coil was used for scanning. The patient was in the supine position, and the scanning range was from the level of the anterior superior iliac spine to the level of the upper femur. The horizontal scanning line was perpendicular to the anal canal, while the coronal and sagittal scanning lines were parallel to the anal canal. The scanning sequence and specific parameters were the same as in the first part of the study.

Region of interest delineation method

The patient's imaging files including T2-weighted imaging (T2WI) were accessed using the open-source software ITK-SNAP (Version 3.6.0, http://www.itksnap.org/). A radiologist with 3 years diagnostic experience in anal fistula manually drew the region of interest (ROI) on the fat suppression T2WI axial position along the rectal and anal canal wall opened by the water sac (Figure 2). The scope of the sketch covered the entire rectal and anal canal wall. If there was any doubt about the sketch, another senior doctor was consulted to reach consensus. The sketched ROI and original image were imported into the Analysis Kit software (version V3.0.0.R, GE Healthcare), which automatically analyzed and calculated the texture feature parameter table of the drawn ROI.

Statistical analysis

The SPSS 22.0 software was used to perform all statistical analysis on the obtained textural feature parameters and detect the normal distribution of the parameters. For normally distributed data, two-tailed independent sample *t*-test was used. For non-normally distributed data, Mann–Whitney U test was used for comparison. $P < 0.05$ was considered to indicate statistical significance. Bivariate Spearman's correlation analysis was conducted on indicators with statistical differences to calculate the redundancy between the textural feature parameters; those with a redundancy threshold > 0.9 were screened out. The receiver operating characteristic (ROC) curve analysis was used to calculate the diagnostic efficacy of each index selected by area under the curve (AUC) comparison, following which the Youden index, specificity, sensitivity, positive likelihood ratio, and negative likelihood ratio of each index were calculated. Finally, binary logistic regression analysis was carried out to identify indicators with statistical differences to establish the logistic regression model of textural feature parameters and calculate the corresponding statistical indicators.

RESULTS

A total of 385 textural feature parameters of the final drawn ROI were calculated by the Analysis Kit software. Of these, 37 parameters showed statistically significant differences in the PFCD group and glandular anal fistula group. Through bivariate Spearman correlation analysis, the redundancy between the feature parameters was calculated, the indicators with a redundancy threshold > 0.9 were filtered

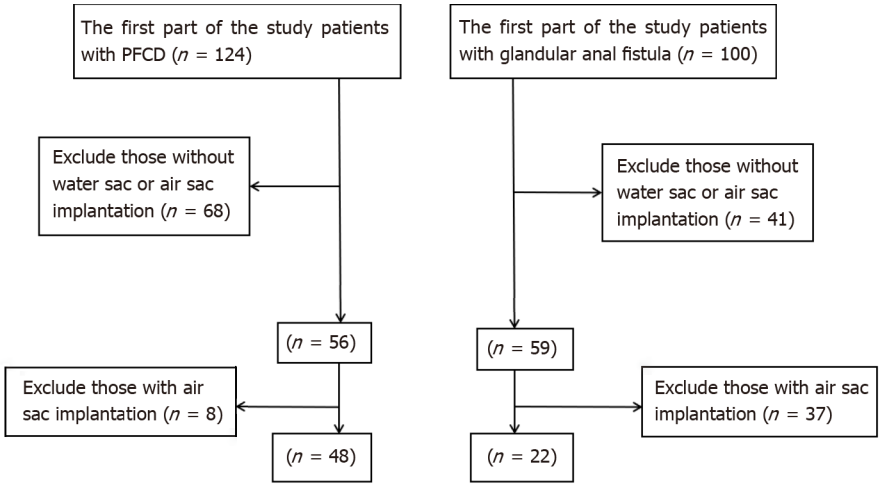

DOI: 10.4240/wjgs.v15.i5.882 **Copyright** ©The Author(s) 2023.

Figure 1 Flow chart of patient inclusion and exclusion. PFCD: Perianal fistulising Crohn's disease.

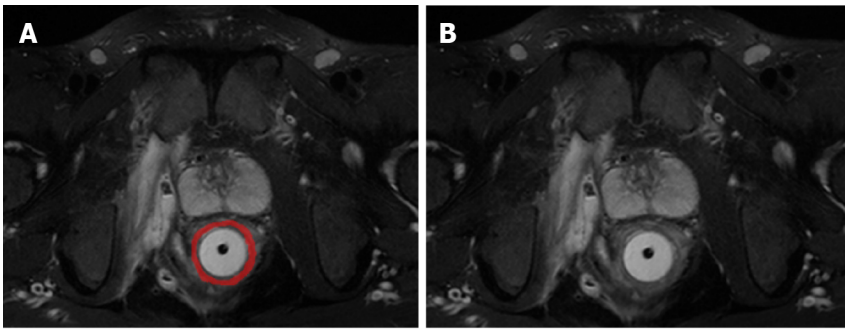

DOI: 10.4240/wjgs.v15.i5.882 **Copyright** ©The Author(s) 2023.

Figure 2 Region of interest sketch diagram. A: The horizontal axis of fat suppression T2-weighted (FS-T2WI) image. The red part is the outlined region of interest. B: The horizontal axis of FS-T2WI image, on the same layer as figure panel A.

out. Finally, 16 textural feature parameters were obtained, including one histogram parameter (histogram-energy); four grey level co-occurrence matrix (GLCM) parameters (GLCM energy_all direction_offset1_SD, GLCM entropy_all direction_offset4_SD, GLCM entropy_all direction_offset7_SD, and Haralick correlation_all direction_offset7_SD); four texture parameters (Correlation_all direction_offset1_SD, cluster prominence_angle 90_offset4, inertia_all direction_offset7_SD, and cluster shade_angle 45_ offset7); five grey level run-length matrix (RLM) parameters (Grey level nonuniformity_ angle 90_offset1, long run emphasis_all direction_offset4_SD, long run high grey level emphasis_all direction _offset1_SD, long run high grey level emphasis_all direction_ offset4_SD, and long run high grey level emphasis_all direction_offset4_SD); and two form factor parameters (surface area and maximum 3D diameter). ROC analysis was carried out for the above texture feature parameters. The AUC of each parameter and its corresponding Youden index, sensitivity, specificity, positive likelihood ratio, and negative likelihood ratio are shown in Table 1. Through binary logistic regression analysis, a logistic regression model of textural feature parameters was established (Table 2). The AUC of the textural feature parameter model was 0.917, and its sensitivity and specificity were 85.42% and 86.36%, respectively. The AUC, sensitivity, and specificity were higher than any individual texture feature parameters (Figure 3, Table 3).

DISCUSSION

The textural feature parameters calculated by the Analysis Kit software were divided into the following six categories: Histogram parameters, texture parameters, form factor parameters, GLCM parameters, grey level RLM parameters, and gray-scale area matrix parameters. Among the 16 parameter indices obtained by statistical analysis in the PFCD group and the glandular anal fistula group, there were two form factor parameters, one histogram parameter, four GLCM parameters, four texture parameters, and five grey level RLM parameters.

Table 1 Receiver operating characteristic curve analysis results of 16 textural feature parameters

Textural feature parameters	AUC	Asymptotic significance level	95%CI	Z statistics	Youden index	Sensitivity	Specificity	+LR	-LR
Histogram parameter									
Histogram-energy	0.670	0.0226	0.547-0.777	2.280	0.3068	62.50	68.18	1.96	0.55
Gray-scale co-occurrence matrix parameters									
GLCM energy_all direction_offset1_SD	0.683	0.0085	0.561-0.789	2.630	0.3087	85.42	45.45	1.57	0.32
GLCM entropy_all direction_offset4_SD	0.664	0.0185	0.541-0.772	2.354	0.3390	52.08	81.82	2.86	0.59
GLCM entropy_all direction_ offset7_SD	0.648	0.0500	0.524-0.758	1.960	0.2992	70.83	59.09	1.73	0.49
Haralick correlation_all direction_offset7 _SD	0.702	0.0027	0.580-0.805	3.005	0.3598	54.17	81.82	2.98	0.56
Texture parameters									
Correlation_all direction_offset1_SD	0.673	0.0126	0.551-0.781	2.496	0.3598	54.17	81.82	2.98	0.56
Cluster prominence_angle 90_offset4	0.648	0.0300	0.524-0.758	2.171	0.3807	56.25	81.82	3.09	0.53
Inertia_all direction_offset7_SD	0.654	0.0397	0.531-0.764	2.057	0.3864	75.00	63.64	2.06	0.39
Cluster shade_angle 45_ offset7	0.648	0.0230	0.524-0.758	2.274	0.3883	47.92	90.91	5.27	0.57
Grey level run-length matrix (RLM) parameters									
Grey level nonuniformity_ angle 90_offset1	0.671	0.0144	0.549-0.779	2.446	0.3598	54.17	81.82	2.98	0.56
Grey level nonuniformity_all direction_offset4_ SD	0.657	0.0243	0.534-0.767	2.253	0.3125	81.25	50.00	0.38	0.62
Long run high grey level emphasis_all direction _offset1_SD	0.728	0.0003	0.609-0.828	3.618	0.3864	75.00	63.64	2.06	0.39
Long run emphasis_all direction_offset4_SD	0.722	0.0013	0.602-0.822	3.222	0.3883	47.92	90.91	5.27	0.57
Long run high grey level emphasis_all direction_ offset4_SD	0.652	0.0391	0.529-0.762	2.063	0.2803	91.67	36.36	1.44	0.23
Form factor parameters									
Surface area	0.728	0.0003	0.609-0.828	3.640	0.3883	47.92	90.91	5.27	0.57
Maximum 3D diameter	0.739	0.0001	0.620-0.836	4.024	0.4337	47.92	95.45	10.54	0.55

AUC: Area under the receiver operating characteristic curve; +LR: Positive likelihood ratio; -LR: Negative likelihood ratio.

The significance of textural feature parameters

Histogram parameters: The histogram represents the properties of a single pixel and describes the distribution of voxel intensity. The first-order statistics included 20 indicators such as energy, entropy, skewness, kurtosis, maximum intensity, minimum intensity, and mean. Among them, energy is a measure of the uniformity of the intensity level distribution, wherein a higher value represents a more uniform intensity level distribution. Entropy is a measure of the randomness of the distribution of coefficient values at intensity levels. A higher entropy value indicates more intense levels of image distribution. That is, the simpler the image, the lower the entropy value, and the more complex the image, the higher the entropy value.

Texture parameters: The texture represents the appearance of the surface and the distribution of its elements, which helps to predict the surface appearance as being either smooth or rough from the image. Correlation refers to the similarity of the gray level of adjacent pixels, indicating the correlation of pixels with their adjacent pixels in the entire image, ranging from -1 to 1. Inertia reflects the clarity and clarity of the image. The degree of depression of the texture can better distinguish the complexity of the grayscale spatial distribution of the lesion area. Cluster prominence reflects the abrupt situation of the image texture: The greater the contrast between the textures, the greater the value. Cluster shade represents the correlation between texture smoothness and symmetry: The higher the value, the less

Table 2 Analysis results of logistic regression model of textural feature parameters

	β coefficient	SE	χ^2 value	Significance	OR	95%CI	
						Lower limit	Upper limit
Inertia_all direction_offset7_SD	-0.004	0.002	3.699	0.054	0.996	0.993	1.000
Cluster shade_angle 45_ offset7	0.000	0.000	7.194	0.007	1.000	1.000	1.000
Long run high grey level emphasis_all direction _offset1_SD	-0.145	0.069	4.351	0.037	0.865	0.755	0.991
Long run emphasis_all direction_offset4_SD	-98.665	56.394	3.061	0.080	0.000	0.000	142353.563
Surface area	0.000	0.000	3.973	0.046	1.000	1.000	1.001
Maximum 3D diameter	-0.121	0.040	8.963	0.003	0.886	0.819	0.959
Constant	9.412	3.758	6.273	0.012	12234.477	-	-

OR: Odds ratio.

Table 3 Receiver operating characteristic curve analysis results of logistic regression model of textural feature parameters

AUC	Asymptotic significance level	95%CI	Z statistics	Youden index	Sensitivity	Specificity	+LR	-LR
0.917	< 0.0001	0.826-0.969	12.645	0.7178	85.42	86.36	6.26	0.17

AUC: Area under the receiver operating characteristic curve; +LR: Positive likelihood ratio; -LR: Negative likelihood ratio.

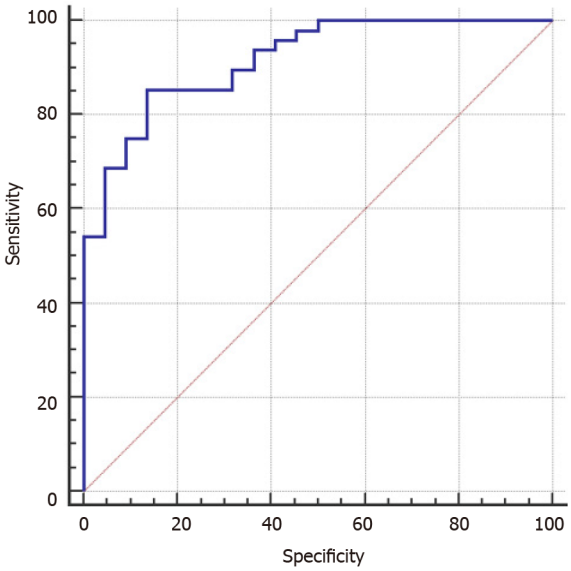

DOI: 10.4240/wjgs.v15.i5.882

Figure 3 Receiver operating characteristic curve of the logistic regression model of textural feature parameters.

smooth and more asymmetric the texture.

Gray level co-occurrence matrix parameters: GLCM represents the joint probability of certain pixels with a certain gray value. By changing the displacement vector between each pair of pixels, the number of joint occurrences of pixels of one gray value and those of another gray value are calculated. The advantage is that it can be spatially correlated in different directions according to the spatial relationship of distance and angle, to fully display the joint information of grayscale and position. Among them, the energy represents the square sum of the elements in GLCM, the range is 0–1, the energy of the unchanged image is 1; and Haralick correlation is to measure the similarity of the gray level of the image in the row or column direction, indicating the local gray correlation. The larger the value, the greater the correlation; the sum entropy can reflect the heterogeneity of the lesion. The greater the sum entropy, the greater the qualitative nature of the disease.

Grey level run-length matrix parameters: RLM is defined as the number and running length of gray scale pixels running in a given direction. The RLM parameters reflect the roughness or smoothness of the image. The larger the long-stroke advantage value, the smoother the image. On the contrary, the larger the short-stroke advantage value, the rougher the image.

Form factor parameters: These describe the three-dimensional size and shape of the ROI[10-12].

The value of textural feature parameters in distinguishing PFCD from glandular anal fistula

Texture analysis is based on image images by quantifying the roughness, regularity, and uniformity of the spatial distribution of pixel gray values in normal tissues and pathological tissues to evaluate the heterogeneity of image signals (including both the heterogeneity that the human eye can and cannot recognize)[3,13]. For MRI images, the gray-scale contrast, uniformity, and texture depth and thickness of the images are important features to distinguish images of lesions from non-lesions[14]. Existing studies have used MRI texture analysis for lesion detection, classification, treatment response evaluation, and prediction of various cancers such as breast cancer, brain tumors, and rectal cancer[15-18]. The statistically different texture feature parameters obtained in this study reflect the uniformity of the distribution of PFCD and glandular anal fistula in the grayscale value of the image, correlation of local gray-scale, roughness of the image, and differences in spatial heterogeneity.

Studies have found that most patients with PFCD are associated with active proctitis. Glandular anal fistula is mostly caused by infection or obstruction of the perianal glands, so it is rarely associated with active proctitis[19]. We conducted a study on the indirect signs of rectal involvement and proctitis in patients with PFCD through texture analysis of the rectal and anal canal wall in patients in the PFCD and glandular anal fistula groups. This study obtained 385 textural feature parameters from the Analysis Kit software, many of which were similar, and some features even had a negative effect on correct classification. The greater the number of features, the higher the complexity and the lower the classification speed, resulting in a reduction in classification accuracy and thus, poor universality[14]. The redundancy of each textural feature parameter was calculated by using the Spearman's correlation analysis and finally 16 textural feature parameters were obtained. The texture feature parameter regression model was obtained by binary logistic regression. The AUC was 0.917, and the calculated sensitivity and specificity was 85.42% and 86.36%, respectively, which was higher than the AUC, sensitivity and specificity of any individual texture feature parameter. We believed that the texture feature parameters had certain discrimination value for PFCD and glandular anal fistula. Although texture analysis is rarely applied to cavity organs such as the rectum or anal canal wall, it is also applied to the analysis of the intestinal wall of Crohn's disease. Makanyanga *et al*[20] applied MRI texture analysis to evaluate the activity of the small intestine in CD, and found that texture feature parameters were correlated with lesion activity. Bhatnagar *et al*[21] found that depending on the presence or absence of histological markers of hypoxia and angiogenesis, the textural feature parameters of the T1-weighted imaging-enhanced image of the small intestine in CD were different. Both local and international literature revealed that there are no studies on the application of image texture analysis to analyze the rectal and anal canal wall of PFCD and glandular anal fistula. Our results likely show that the texture feature parameters are of certain significance for the differential diagnosis of PFCD and glandular anal fistula.

Limitations and perspective

First, owing to the thin wall of the rectum and anal canal, it is difficult to delineate the ROI. In this study, filling the rectum and anal canal with water sacs was used to increase the contrast with the surrounding tissue to reduce the error. Second, because of the small sample size in this study, there was no separate verification set to validate the textural feature parameter model of this study. Further studies with larger sample size are needed to increase the stability of the textural feature parameter and verify the model. Meanwhile, the PFCD group included in this study contains a mix of patients with and without active proctitis. In the future, texture analysis should be used to further investigate whether there are differences between the two subgroups. Third, a primary issue with regard to the texture field is the decipherer of the texture features in a context, even though they were somehow validated[22].

CONCLUSION

In conclusion, the textural feature parameters obtained from the texture analysis of the rectal and anal canal wall in the PFCD group and glandular anal fistula group has some identification value for these two lesions, and can be used as a reference index for imaging specialists to identify and distinguish these two lesions.

ARTICLE HIGHLIGHTS

Research background

Perianal fistulising Crohn's disease (PFCD) and glandular anal fistula have many similarities on conventional magnetic resonance imaging (MRI); therefore, it is difficult to differentiate these conditions in the early stages with conventional MRI. Texture analysis based on conventional MRI images can quantitatively analyze image pixel information and reflect the internal heterogeneity and pathological characteristics of the lesion.

Research motivation

This study aimed to analyze the texture of the rectum and anal canal wall in the PFCD group and glandular anal fistula group to explore whether the texture feature parameters are valuable in identifying and differentiating these two lesions, which provides a non-invasive method for preoperatively differentiating these two entities.

Research objectives

Therefore, the purpose of this study is to differentiate PFCD from glandular anal fistula using MRI texture analysis.

Research methods

Patients with rectal water sac implantation were screened from the first part of this study (48 patients with PFCD and 22 patients with glandular anal fistula). Open-source software ITK-SNAP (Version 3.6.0, http://www.itksnap.org/) was used to delineate the region of interest (ROI) of the entire rectum and anal canal wall on every axial section, and then the ROIs were input in the Analysis Kit software (version V3.0.0.R, GE Healthcare) to calculate the textural feature parameters. Textural feature parameter differences were compared between the two groups and selected for further analysis.

Research results

In all, 385 textural parameters were obtained, including 37 parameters with statistically significant differences between the PFCD and glandular anal fistula groups. Then, 16 texture feature parameters remained after bivariate Spearman correlation analysis, including one histogram parameter; four grey level co-occurrence matrix (GLCM) parameters; four texture parameters; five grey level run-length matrix (RLM) parameters; and two form factor parameters. The AUC, sensitivity, and specificity of the model of textural feature parameters were 0.917, 85.42%, and 86.36%, respectively.

Research conclusions

The model of textural feature parameters showed good diagnostic performance for PFCD. The texture feature parameters of the rectum and anal canal in fat suppression T2-weighted imaging are helpful to distinguish PFCD from glandular anal fistula.

Research perspectives

This study provides a non-invasive method (MRI texture analysis) to preoperatively differentiate PFCD from glandular anal fistula, which has a profound clinical significance in guiding treatment strategy and predicting prognosis for patients with PFCD and anal fistula.

ACKNOWLEDGEMENTS

We thank our colleagues for their continuous and excellent support.

FOOTNOTES

Author contributions: Zhu X designed the research study; Ye DD, Li J, and Liu SW performed the research; Zhu X and Wang JH analyzed the data and wrote the manuscript; All authors have read and approve the final manuscript.

Institutional review board statement: This study was approved by the institutional review board of the Affiliated Hospital of Nanjing University of Chinese Medicine; informed consent was waived owing to the retrospective nature of the study.

Conflict-of-interest statement: All the authors report no relevant conflicts of interest for this article.

Data sharing statement: All datasets generated for this study are included in the manuscript and/or the

supplementary files.

Country/Territory of origin: China

ORCID number: Xin Zhu 0000-0001-5393-9220; Dan-Dan Ye 0000-0002-7458-1341; Jian-Hua Wang 0000-0001-5874-2080; Jing Li 0000-0001-9663-4670; Shao-Wei Liu 0000-0003-0529-1188.

S-Editor: Li L
L-Editor: A
P-Editor: Wu RR

REFERENCES

1 **Torres J**, Mehandru S, Colombel JF, Peyrin-Biroulet L. Crohn's disease. *Lancet* 2017; **389**: 1741-1755 [PMID: 27914655 DOI: 10.1016/S0140-6736(16)31711-1]
2 **Schwartz DA**, Ghazi LJ, Regueiro M, Fichera A, Zoccali M, Ong EM, Mortelé KJ; Crohn's & Colitis Foundation of America, Inc. Guidelines for the multidisciplinary management of Crohn's perianal fistulas: summary statement. *Inflamm Bowel Dis* 2015; **21**: 723-730 [PMID: 25751066 DOI: 10.1097/MIB.0000000000000315]
3 **Lubner MG**, Smith AD, Sandrasegaran K, Sahani DV, Pickhardt PJ. CT Texture Analysis: Definitions, Applications, Biologic Correlates, and Challenges. *Radiographics* 2017; **37**: 1483-1503 [PMID: 28898189 DOI: 10.1148/rg.2017170056]
4 **Kim JH**, Ko ES, Lim Y, Lee KS, Han BK, Ko EY, Hahn SY, Nam SJ. Breast Cancer Heterogeneity: MR Imaging Texture Analysis and Survival Outcomes. *Radiology* 2017; **282**: 665-675 [PMID: 27700229 DOI: 10.1148/radiol.2016160261]
5 **Imbriaco M**, Cuocolo R. Does Texture Analysis of MR Images of Breast Tumors Help Predict Response to Treatment? *Radiology* 2018; **286**: 421-423 [PMID: 29356631 DOI: 10.1148/radiol.2017172454]
6 **Chamming's F**, Ueno Y, Ferré R, Kao E, Jannot AS, Chong J, Omeroglu A, Mesurolle B, Reinhold C, Gallix B. Features from Computerized Texture Analysis of Breast Cancers at Pretreatment MR Imaging Are Associated with Response to Neoadjuvant Chemotherapy. *Radiology* 2018; **286**: 412-420 [PMID: 28980886 DOI: 10.1148/radiol.2017170143]
7 **Mulé S**, Thiefin G, Costentin C, Durot C, Rahmouni A, Luciani A, Hoeffel C. Advanced Hepatocellular Carcinoma: Pretreatment Contrast-enhanced CT Texture Parameters as Predictive Biomarkers of Survival in Patients Treated with Sorafenib. *Radiology* 2018; **288**: 445-455 [PMID: 29584597 DOI: 10.1148/radiol.2018171320]
8 **Yin JD**, Song LR, Lu HC, Zheng X. Prediction of different stages of rectal cancer: Texture analysis based on diffusion-weighted images and apparent diffusion coefficient maps. *World J Gastroenterol* 2020; **26**: 2082-2096 [PMID: 32536776 DOI: 10.3748/wjg.v26.i17.2082]
9 **Chen Y**, Li H, Feng J, Suo S, Feng Q, Shen J. A Novel Radiomics Nomogram for the Prediction of Secondary Loss of Response to Infliximab in Crohn's Disease. *J Inflamm Res* 2021; **14**: 2731-2740 [PMID: 34194236 DOI: 10.2147/JIR.S314912]
10 **Yu H**, Buch K, Li B, O'Brien M, Soto J, Jara H, Anderson SW. Utility of texture analysis for quantifying hepatic fibrosis on proton density MRI. *J Magn Reson Imaging* 2015; **42**: 1259-1265 [PMID: 26477447 DOI: 10.1002/jmri.24898]
11 **Li Z**, Mao Y, Huang W, Li H, Zhu J, Li W, Li B. Texture-based classification of different single liver lesion based on SPAIR T2W MRI images. *BMC Med Imaging* 2017; **17**: 42 [PMID: 28705145 DOI: 10.1186/s12880-017-0212-x]
12 **Chaddad A**, Tanougast C. Extracted magnetic resonance texture features discriminate between phenotypes and are associated with overall survival in glioblastoma multiforme patients. *Med Biol Eng Comput* 2016; **54**: 1707-1718 [PMID: 26960324 DOI: 10.1007/s11517-016-1461-5]
13 **Sidhu HS**, Benigno S, Ganeshan B, Dikaios N, Johnston EW, Allen C, Kirkham A, Groves AM, Ahmed HU, Emberton M, Taylor SA, Halligan S, Punwani S. "Textural analysis of multiparametric MRI detects transition zone prostate cancer". *Eur Radiol* 2017; **27**: 2348-2358 [PMID: 27620864 DOI: 10.1007/s00330-016-4579-9]
14 **Guo CG**, Ren S, Chen X, Wang QD, Xiao WB, Zhang JF, Duan SF, Wang ZQ. Pancreatic neuroendocrine tumor: prediction of the tumor grade using magnetic resonance imaging findings and texture analysis with 3-T magnetic resonance. *Cancer Manag Res* 2019; **11**: 1933-1944 [PMID: 30881119 DOI: 10.2147/CMAR.S195376]
15 **Su CQ**, Lu SS, Han QY, Zhou MD, Hong XN. Intergrating conventional MRI, texture analysis of dynamic contrast-enhanced MRI, and susceptibility weighted imaging for glioma grading. *Acta Radiol* 2019; **60**: 777-787 [PMID: 30244590 DOI: 10.1177/0284185118801127]
16 **Parikh J**, Selmi M, Charles-Edwards G, Glendenning J, Ganeshan B, Verma H, Mansi J, Harries M, Tutt A, Goh V. Changes in primary breast cancer heterogeneity may augment midtreatment MR imaging assessment of response to neoadjuvant chemotherapy. *Radiology* 2014; **272**: 100-112 [PMID: 24654970 DOI: 10.1148/radiol.14130569]
17 **Meng Y**, Zhang C, Zou S, Zhao X, Xu K, Zhang H, Zhou C. MRI texture analysis in predicting treatment response to neoadjuvant chemoradiotherapy in rectal cancer. *Oncotarget* 2018; **9**: 11999-12008 [PMID: 29552288 DOI: 10.18632/oncotarget.23813]

18 **De Cecco CN**, Ganeshan B, Ciolina M, Rengo M, Meinel FG, Musio D, De Felice F, Raffetto N, Tombolini V, Laghi A. Texture analysis as imaging biomarker of tumoral response to neoadjuvant chemoradiotherapy in rectal cancer patients studied with 3-T magnetic resonance. *Invest Radiol* 2015; **50**: 239-245 [PMID: 25501017 DOI: 10.1097/RLI.0000000000000116]

19 **Tougeron D**, Savoye G, Savoye-Collet C, Koning E, Michot F, Lerebours E. Predicting factors of fistula healing and clinical remission after infliximab-based combined therapy for perianal fistulizing Crohn's disease. *Dig Dis Sci* 2009; **54**: 1746-1752 [PMID: 19003531 DOI: 10.1007/s10620-008-0545-y]

20 **Makanyanga J**, Ganeshan B, Rodriguez-Justo M, Bhatnagar G, Groves A, Halligan S, Miles K, Taylor SA. MRI texture analysis (MRTA) of T2-weighted images in Crohn's disease may provide information on histological and MRI disease activity in patients undergoing ileal resection. *Eur Radiol* 2017; **27**: 589-597 [PMID: 27048528 DOI: 10.1007/s00330-016-4324-4]

21 **Bhatnagar G**, Makanyanga J, Ganeshan B, Groves A, Rodriguez-Justo M, Halligan S, Taylor SA. MRI texture analysis parameters of contrast-enhanced T1-weighted images of Crohn's disease differ according to the presence or absence of histological markers of hypoxia and angiogenesis. *Abdom Radiol (NY)* 2016; **41**: 1261-1269 [PMID: 26867730 DOI: 10.1007/s00261-016-0657-3]

22 **Ren S**, Zhao R, Zhang J, Guo K, Gu X, Duan S, Wang Z, Chen R. Diagnostic accuracy of unenhanced CT texture analysis to differentiate mass-forming pancreatitis from pancreatic ductal adenocarcinoma. *Abdom Radiol (NY)* 2020; **45**: 1524-1533 [PMID: 32279101 DOI: 10.1007/s00261-020-02506-6]

Published by **Baishideng Publishing Group Inc**
7041 Koll Center Parkway, Suite 160, Pleasanton, CA 94566, USA
Telephone: +1-925-3991568
E-mail: bpgoffice@wjgnet.com
Help Desk: https://www.f6publishing.com/helpdesk
https://www.wjgnet.com